Biochimica et Biophysica Acta 1848 (2015) 203–210

Contents lists available at ScienceDirect

Biochimica et Biophysica Acta

journal homepage: www.elsevier.com/locate/bbamem

Delineation of the dynamic properties of individual lipid species in native and synthetic pulmonary surfactants☆

Suzanne Farver [a,1], Adam N. Smith [b], Frank D. Mills [a], Adam G. Egri [a], Joanna R. Long [a,*,2]

[a] Department of Biochemistry and Molecular Biology, University of Florida, Gainesville, FL 32610, USA
[b] Department of Chemistry, University of Florida, Gainesville, FL 32611, USA

ARTICLE INFO

Article history:
Received 17 February 2014
Received in revised form 20 April 2014
Accepted 4 May 2014
Available online 20 May 2014

Keywords:
Pulmonary surfactant
Surfactant protein B
Lipid dynamics
Membrane-active peptide
^{2}H NMR
Respiratory distress syndrome

ABSTRACT

Pulmonary surfactant (PS) is characterized by a highly conserved lipid composition and the formation of unique multilamellar structures within the lung. An unusually high concentration of DPPC is a hallmark of PS and is critical to the formation of a high surface area, stable air/water interface; the unusual lipid polymorphisms observed in PS are dependent on surfactant proteins, particularly lung surfactant protein B (SP-B). The molecular mechanisms of lipid trafficking and assembly in PS remain largely uncharacterized. Using ^{2}H and ^{31}P NMR, we characterize the dynamics and polymorphisms of the major lipid species in native PS and synthetic lipid mixtures as a function of SP-$B_{1\text{-}25}$ addition. Our findings point to increased dynamics and a departure from a lamellar behavior for DPPC on addition of the peptide, consistent with our observations of DPPC phase separation in native surfactant. The monounsaturated lipids POPC, POPG and POPE remain in a lamellar phase and are less affected than DPPC by surfactant peptide addition. Additionally, we demonstrate that the properties of a native PS can be successfully mimicked by using a fully synthetic lipid mixture allowing the efficient evaluation of peptidomimetics under development for PS replacement therapies via NMR spectroscopy. The specificity of the dynamic changes in DPPC relative to POPC suggests the importance of tuning partitioning properties in successful peptidomimetic design. This article is part of a Special Issue entitled: NMR Spectroscopy for Atomistic Views of Biomembranes and Cell Surfaces. Guest Editors: Lynette Cegelski and David P. Weliky.

1. Introduction

Mammals require high oxygen uptake, which is facilitated by the large inner surface area of the lung at 300 cm^2 per cubic centimeter [1]. A lipid/protein complex known as pulmonary surfactant (PS) lines the inside of the alveoli and reduces the work of breathing by minimizing surface tension [2]. Respiratory Distress Syndrome (RDS) occurs in premature infants, who produce inadequate amounts of PS, as well as in older children, due to low PS activity caused by lung injury [3]. PS is synthesized, processed, stored, secreted, and recycled by type II pneumocytes. It is secreted to the alveolar subphase as specialized organelles known as lamellar bodies (LB) and recycled every 5–10 h. Secreted LB can fuse to form tubular myelin (TM) while some LB maintain their packed structure; both TM and LB contribute to the in vivo formation of the interfacial film important for oxygen exchange by unraveling and adsorbing onto the air/water interface [4]. The molecular level processes by which PS lipids are trafficked to the air/water interface have been explored in several recent in vitro studies [5–9]. A fully saturated, surface stable phospholipid, dipalmitoylphosphatidylcholine (DPPC), found at high levels in PS, is thought to be the major component of the surface film; whether it is specifically trafficked to the interface or most of the non-DPPC components of PS are squeezed out during the compression/expansion cycles leaving a DPPC-rich surface film or a combination of these processes occur in the PS cycle in vivo is unknown [4]. The molecular level details of the unusual dynamics and organization of LB and TM in the aqueous phase also remain poorly characterized.

PS is an ideal system for studying the molecular basis of protein mediated lipid trafficking and/or assembly in an aqueous environment. Its simple lipid and protein composition (relative to the plasma membrane) is highly conserved among mammalian species, with lipids making up >90% of the LB and TM. A summary of the lipids found in PS is presented

Abbreviations: PS, pulmonary surfactant; CLSE, calf lung surfactant extract; SP-B, surfactant protein B; MLV, multilamellar vesicle; RDS, respiratory distress syndrome; DPPC, 1, 2-dipalmitoyl-*sn*-glycero-3-phosphatidylcholine; DPPC-d_{62}, 1,2-d_{62}-dipalmitoyl-*sn*-glycero-3-phosphatidylcholine; P/L, peptide/lipid molar ratio; POPC, 1-palmitoyl-2-oleoyl-*sn*-glycero-3-phosphatidylcholine; POPC-d_{31}, 1-d_{31}-palmitoyl-2-oleoyl-*sn*-glycero-3-phosphatidylcholine; POPG, 1-palmitoyl-2-oleoyl-*sn*-glycero-3-phosphatidylglycerol; POPG-d_{31}, 1-d_{31}-palmitoyl-2-oleoyl-*sn*-glycero-3-phosphatidylglycerol; POPE, 1-palmitoyl-2-oleoyl-*sn*-glycero-3-phosphatidylethanolamine; POPE-d_{31}, 1-d_{31}-palmitoyl-2-oleoyl-*sn*-glycero-3-phosphatidylethanolamine; Chol, cholesterol

☆ This article is part of a Special Issue entitled: NMR Spectroscopy for Atomistic Views of Biomembranes and Cell Surfaces.

* Corresponding author.
E-mail address: jrlong@mbi.ufl.edu (J.R. Long).
[1] Current address: Department of Chemistry and Physics, Troy University, Troy, AL 36082, USA.
[2] Tel.: +1 352 846 1506.

http://dx.doi.org/10.1016/j.bbamem.2014.05.012
0005-2736/

in Table 1 [4,10–12]. Zwitterionic phospholipids (primarily phosphatidylcholines) make up ~85% of total PS phospholipids; almost half of the phosphatidylcholine component is 1, 2-dipalmitoyl-*sn*-glycero-3-phosphocholine (DPPC). The two saturated acyl chains of DPPC enable it to be packed tightly in the monolayer at the air/water interface; the stability of DPPC monolayers to lateral pressure during compression is thought to be critical to the integrity of this interface in the lung. The melting temperature of neat DPPC is 41 °C; the remaining PC lipids are monounsaturated and likely increase the fluidity of the DPPC rich PS, accelerating lipid trafficking and surface film formation [11]. While LB and TM are primarily lamellar, they do not have the same fluid consistency as cell membranes and their multilamellar structures are packed more tightly together than is typically observed for other lipid assemblies (e.g. intracellular organelles); it has been hypothesized that non-lamellar polymorphisms, such as the cubic or hexagonal phases, may play a crucial role in the organization and function of PS [13].

Although lipids underpin the macromolecular assemblies important to PS function, their unique properties are dependent on low levels of surfactant proteins. In particular, surfactant protein B (SP-B), which is highly hydrophobic and present at low levels (<2% by weight), is critical to LB/TM integrity and the formation of a viable air/water interface [14,15]. Humans with genetic SP-B dysfunction die soon after birth as do genetically engineered SP-B null mice. SP-B is a particularly challenging protein to produce or isolate due to its high hydrophobicity, so animal sources of PS are commonly used in treating RDS, posing a risk of infection or immune response [16]. In particular, calf lung surfactant extract (CLSE) is a surfactant replacement therapy prepared from chloroform extracts of lavaged PS from calf lungs [2]. It is commonly administered to premature infants with RDS under the name *Infasurf*. The lipids in CLSE are unusually surface active and form unique aqueous assemblies similar to native PS due to low levels of surfactant proteins SP-B and SP-C. CLSE contains 93% phospholipid, 5% cholesterol and neutral lipids, and 2% SP-B and SP-C by weight and thus closely mimics human PS.

Given the tremendous importance of SP-B to PS function, surfactant replacement methods employing simple surface-active peptide analogs of SP-B have also been investigated as they can be easily produced with high yield and purity. SP-B_{1-25} is an amphipathic peptide composed of the first 25 amino acids of the N-terminus of SP-B which retains much of the biological activity of full length SP-B and is more resistant to inhibition by plasma proteins infiltrating the lung during injury [17–22]. Understanding how it functions in the PS lipid environment would allow the development of mimetics which are even more stable. CD and FTIR indicate the presence of helical structure in the C-terminal portion of SP-B_{1-25} when it is associated with lipid monolayers [20]; the very hydrophobic N-terminal tail of SP-B_{1-25} enables rapid insertion into lipid films [8]. Previously we have shown that the first several amino acids are critical to the induction of uncommon lipid polymorphisms by SP-B_{1-25} in synthetic binary lipid systems with distinct differences between DPPC/POPG and POPC/POPG mixtures [9]. These results led us to study lipid polymorphisms in more complex lipid mixtures, including therapeutic CLSE, to gain a deeper understanding of lipid behavior in PS.

The goals of this study are threefold: 1) to individually characterize the dynamics of the major lipid species in therapeutic CLSE, 2) to compare lipid dynamics in CLSE to a completely synthetic lipid system based on PS composition, and 3) to examine how lipid dynamics and organization are affected by the addition of the PS peptide SP-B_{1-25} via ^{31}P and ^{2}H static ssNMR experiments. ^{31}P spectroscopy allows monitoring of lipid dynamics and polymorphisms for all lipid species in a given sample while ^{2}H spectroscopy allows monitoring of the dynamics and polymorphisms of individual lipid species that are deuterium enriched and in particular the dynamics of the deuterated lipid acyl chains.

Table 1
Lipid composition of native PS and lipid mixtures used in this study.

	Phospholipid composition (%total) [% disaturated]								Cholesterol
Source	PC	LPC	SM	PG	PI	PS	PE	LBPA	(%chol/PL)
Human	80.5 [47.7]	Tr	2.7	9.1	2.6	0.9	12.3	NR	7.3
Bovine	79.2 [49.9]	Tr	Tr	11.3 [33.3]	1.8	Tr	3.5	2.6	3
$CLSE^{T}$	>75 [>60]	NR	NR	NR	NR	NR	NR	NR	NR
$CSLE^{S}$	76.2 [62.5]	–	–	14.3	–	–	9.5	–	9.5

2. Materials & methods

2.1. Materials

DPPC, POPC, POPG, POPE, DPPC-d_{62}, POPC-d_{31}, POPG-d_{31} and POPE-d_{31} were purchased as chloroform solutions from Avanti Polar Lipids (Alabaster, AL) and quantified by phosphate analysis (Bioassay Systems, Hayward, CA); cholesterol in powder form was also purchased from Avanti. Research grade calf lung surfactant extract (CLSE) was generously provided as a gift from ONY, Inc. (Amherst, NY). CLSE is a chloroform extract of natural surfactant from calf lungs manufactured by ONY, Inc., as the pharmaceutical drug product *Infasurf*. Upon receipt, the chloroform was evaporated and CLSE was lyophilized for longer storage stability. CLSE contains 93–101 mg/ml of total phospholipid and ~1.3 and ~0.7 mg/ml of surfactant proteins B and C (SP-B and SP-C), respectively. Unless otherwise stated, other reagents were purchased from Fisher Scientific (Hampton, NH) and used as received.

2.2. Biochemical separation of CLSE lipids and proteins

To make samples of CLSE lacking surfactant proteins, the proteins were separated from the lipids by gel permeation chromatography with a Sephadex LH-20 (GE Healthcare) resin and 95:95:10 chloroform:methanol:0.1 N HCl (v/v/v) as the running solvent using previously established methods [23]. Eluent fractions were assayed by phosphate and protein analyses. Inorganic phosphate was liberated from the phospholipids and quantified to determine phospholipid concentration via a colorimetric assay (Bioassay systems) [24]. Protein content was assayed via the Amido Black Protein Assay [25,26]. These assays are sensitive to μg quantities and were used to monitor the separation. Fractions containing only protein or only phospholipid were separately pooled and extracted into chloroform to remove acid; fractions containing both lipids and proteins were pooled, concentrated and run over the column a second time. Phosphate and protein assays indicated successful separation of CLSE lipids and proteins after a second pass through the column. Due to the small, undetectable concentration of cholesterol in the tail end of the eluent with each run, the column was flushed with an additional volume of chloroform:methanol:0.1 N HCl at the end of each separation to recover the cholesterol. Concentrated cholesterol was identified by TLC and the collected cholesterol was added to the phospholipid fractions. The combined lipid fractions were dried with nitrogen gas and then lyophilized from cyclohexane. Actual lipid concentrations for the purpose of making NMR samples were determined after combining all lipid fractions from every pass through the column. The amount of protein isolated was too small for the purposes of this study and was not used further.

2.3. Preparation of synthetic lipid mixtures

A synthetic PS lipid system was also studied for comparison to CLSE and earlier studies of the binary mixture 4:1 DPPC/POPG [7–9]. The phospholipids were purchased as chloroform solutions and mixed after verifying their concentrations by phosphate analysis (Bioassay Systems, Hayward, CA). Cholesterol was obtained as a dry powder and dissolved in chloroform. Appropriate volumes of lipid chloroform solutions were mixed to give final lipid molar ratios of 10:6:3:2:2 DPPC/POPC/POPG/POPE/chol for the synthetic PS lipid mixture, denoted $CLSE^{S}$.

2.4. Synthesis of SP-B_{1-25}

SP-B_{1-25}, (FPIPLPYCWLCRALIKRIQAMIPKG) was synthesized via solid-phase peptide synthesis, purified by RP-HPLC, and verified by mass spectrometry (m/z = 2928). To ensure that only peptide monomers were present, TCEP was added to the peptide in methanol and the monomeric peptide was isolated by using size-exclusion chromatography. The monomer was then diluted into ammonium acetate, pH 8, and oxidized overnight; a purely monomeric peptide solution was verified by non-reducing SDS-PAGE gel analysis. The peptide solution was then lyophilized and dissolved in methanol to yield a ~1 mM stock solution and quantitated by UV analysis.

2.5. Preparation of NMR samples

Samples were made with therapeutic CLSE (as received from ONY with both lipids and proteins present, denoted $CLSE^T$), CLSE lipids after removal of proteins ($CLSE^L$), and by combining pure lipids in chloroform based on the lipid composition of CLSE ($CLSE^S$). Acyl chain deuterated lipids, DPPC-d_{62}, POPC-d_{31}, POPG-d_{31}, and POPE-d_{31}, were added to the CLSE and synthetic lipid mixtures as reporters in the ^2H NMR experiments. The animal derived PS samples contained 20–50 mg of CLSE (lipids only for $CLSE^L$ or with SP-B and SP-C also present for $CLSE^T$) with 2–5 mg added deuterated phospholipid (e.g. 10% of total lipids). For peptide containing samples, SP-B_{1-25} in methanol was added to the lipid chloroform solutions resulting in P/L ratios ranging from 1:100 to 1:20. Samples were dried under a stream of nitrogen while in a water bath at 45–50 °C; the resulting films were suspended in warm cyclohexane (45–50 °C), flash frozen in nitrogen, and lyophilized overnight to remove residual solvent. For each solid-state NMR sample, ~15–50 mg of peptide–lipid powder was placed in a 5 mm diameter NMR tube and 200 μL of buffer containing 50 mM HEPES, pH 7.4, 140 mM NaCl, and 1 mM EDTA in ^2H depleted water (Cambridge Isotopes, Andover MA) was added. The hydrated dispersions (in NMR tubes) were subjected to 5 freeze–thaw cycles with gentle vortexing to form MLVs.

2.6. Solid state NMR analysis

^{31}P and ^2H NMR data were collected on a 500 MHz Bruker DRX system (Billerica, MA) with a 5 mm BBO probe. A temperature calibration using methanol and ethylene glycol standards was performed before data collection; variable temperature spectra for POPC and DPPC standards containing 10% deuterated lipid confirmed the calibration with phase transitions at −2 and 41 °C, respectively. For the ^{31}P NMR experiments, spectra were collected by using a Bloch decay pulse sequence to minimize T_2 relaxation effects due to lipid dynamics, with 25 kHz proton decoupling applied during signal acquisition. ^{31}P Spectra were acquired with 256–512 scans and a 5 s recycle delay between scans to minimize RF sample heating. The ^{31}P B_1 field was 52 kHz (4.85 μs 90° pulse). ^2H NMR spectra were collected by using a quad echo sequence (90°-τ-90°-τ-acq with τ = 30 μs) with a ^2H B_1 field of 42 kHz (5.95 μs 90° pulse). ^2H spectra were acquired with 2 k–16 k scans and a 0.5 s recycle delay between scans. Depaking of NMR data was accomplished with previously published algorithms which simultaneously dePake and determine macroscopic ordering in partially aligned lipid spectra using Tikonov regularization [27]. Assignments of ^2H resonances were based on Petrache et al. [28].

3. Results

3.1. The major lipids in CLSE exhibit lamellar properties at physiologic temperatures; DPPC has a higher melting temperature than the monounsaturated lipids

$CLSE^T$ (therapeutic CLSE as received without any purification) was combined with low levels of deuterated lipid to probe the behavior of individual lipid species within the CLSE environment, which includes SP-B and SP-C. ^2H and ^{31}P NMR spectra of DPPC-d_{62}, POPC-d_{31}, POPG-d_{31}, and POPE-d_{31} containing $CLSE^T$ (i.e. four separate samples) were collected over a range of temperatures (Fig. 1 and Supplementary Figures S-1 and S-2). A series of variable temperature ^{31}P NMR spectra were also collected on a $CLSE^T$ sample that did not have any deuterated lipid added (Figure S-2); the properties of this sample were indistinguishable from the samples containing deuterated lipids, verifying that addition of small amounts of deuterated lipid does not change the phase behavior of $CLSE^T$. The phase transition temperatures of the individual lipid species were determined by fitting first-moment analyses of ^2H NMR spectra collected every 5 °C over the range of −10 to 55 °C (Table 2 and Figure S-1). The phase transitions are significantly broader than in pure lipid systems, in part due to the presence of cholesterol, and agree with previous measurements of PS thermal behavior by differential scanning calorimetry [29]. While the phase transition temperature of DPPC is much lower in $CLSE^T$ compared to the pure lipid (28 vs. 41 °C), it still melts at considerably higher temperature than the mono-unsaturated lipids, suggesting some phase separation in $CLSE^T$ of DPPC-enriched domains. The T_m values for POPC, POPG, and POPE are similar, at 19–22 °C, and they exhibit similarly broad melting ranges suggesting that they are well mixed; their significantly higher T_m relative to neat POPC or POPG suggests some mixing with DPPC and other high melting species such as saturated fatty acids. At a physiologic temperature, all the lipids exhibit typical lamellar, liquid–crystalline lineshapes. The dePaked ^2H spectra at 40 °C for the $CLSE^T$ samples containing deuterated lipids (Fig. 2) show greater order for DPPC-d_{62} acyl chains compared to POPC-d_{31}, POPG-d_{31} and POPE-d_{31}, consistent with its high melting temperature. Order parameter plots comparing the various lipids are provided in Figure S-3.

3.2. The dynamics of the major lipids in CLSE are unchanged by protein removal

The protein components of CLSE were removed via gel permeation chromatography, and the lipid constituents of CLSE, denoted $CLSE^L$, were combined with individually deuterated lipids and again examined by ^2H and ^{31}P NMR spectroscopy. The thermal behavior of the lipids in $CLSE^L$, as reported by ^2H and ^{31}P NMR measurements (Figs. 1 and Supplementary Information), is remarkedly similar to that observed in $CLSE^T$ with DPPC melting at 28 °C in both preparations and the order parameter profiles for the individual lipid species agreeing within the error bars of the measurements (Figures S-3 and S-4). The ^{31}P data indicate a slightly larger fraction of lysophosphatidylcholine (LPC) lipid species present, as evidenced by an isotropic resonance at 0 ppm, in the $CLSE^L$ samples compared to the $CLSE^T$ samples (Figure S-5), likely due to using two separate batches of CLSE from ONY leading to small differences in the amount of lysolipids present. Small differences are also seen between the spectra of the mono-unsaturated lipids in the two preparations, but these primarily arise from differences in bulk alignment of the lipid vesicles in the high magnetic field, which is very sensitive to sample hydration, rather than differences in lipid dynamics at the molecular level. Depaked spectra, which correct for any changes in bulk alignment, are identical between the two CLSE preparations (Fig. 2).

3.3. The lipid properties of CLSE are closely matched by a synthetic PS lipid mixture

CLSE was also compared to a fully synthetic lipid mixture, denoted $CLSE^S$ (Table 1), containing lipid concentrations mirroring the major lipids of CLSE (DPPC, POPC, POPG, POPE, and cholesterol), which allows full knowledge of the lipid composition in the sample and better control of relative concentrations. ^2H and ^{31}P NMR measurements (Figs. 1 and S-6) indicate that in the fluid phase the properties of the individually deuterated lipid species mirror those of the deuterated lipids added to $CLSE^T$ and $CLSE^L$ with identical ordering of the acyl chains. However,

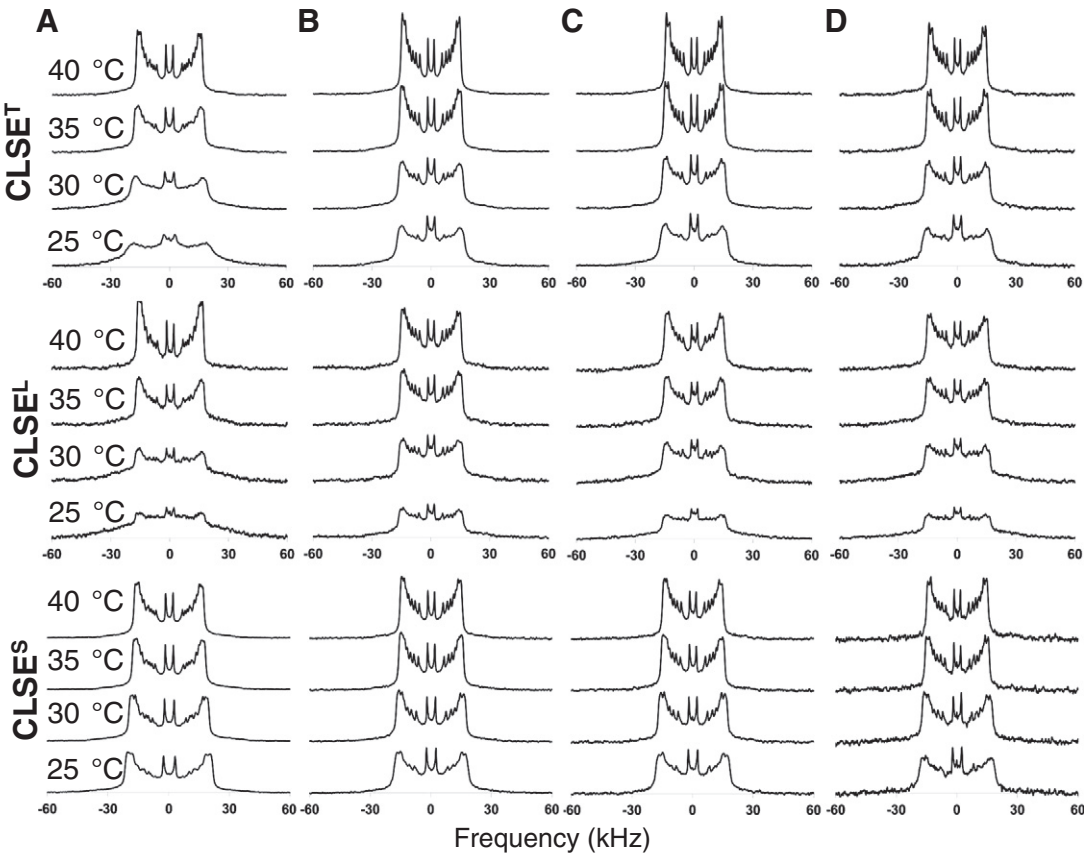

Fig. 1. Deuterium NMR spectra for CLSE samples containing low reporter levels of A) DPPC-d_{62}, B) POPC-d_{31}, C) POPG-d_{31}, and D) POPE-d_{31} obtained at the indicated temperatures. The top row is from samples made with native CLSE (containing low levels of SP-B and SP-C), the middle row is after removal of the proteins from CLSE, and the bottom row is a synthetic mixture of lipids designed to mimic the lipid composition of CLSE. The mono-unsaturated lipids exhibit a lower melting temperature compared to DPPC in the native CLSE regardless of protein content. In the synthetic lipid mixture, less phase separation of DPPC is observed.

all the lipids, including DPPC, are observed to be fully in the liquid crystalline phase at 25 °C, suggesting that there is no phase separation in the synthetic system at lower temperatures and that minor, non-protein species in $CLSE^T$ and $CLSE^L$ are facilitating phase separation of DPPC. Nonetheless, the bulk properties of $CLSE^S$ are very similar, as shown by ^{31}P NMR measurements (Figure S-6), as are the dynamics of the individual lipid species at physiologic temperatures. Notably, the dePaked spectra of DPPC-d_{62} in $CLSE^S$, $CLSE^L$, and $CLSE^T$ environments at 40 °C are indistinguishable (Fig. 2).

3.4. Addition of SP-$B_{1\text{-}25}$ to CLSE lipids specifically alters the phase properties of DPPC

$CLSE^T$ preparations contain very low concentrations of SP-B and SP-C, as does human PS. Given the low concentrations of these proteins, it is likely that their effects on the collective dynamics of the lipids are minimal since there are approximately 400–800 lipid molecules for each SP-C or SP-B monomer [30]. Nonetheless, the possibility exists that the proteins are trafficking a small percentage of lipids in the bulk lamellar sample, which is undetectable via the solid-state NMR experiments. However, a larger P/L ratio could make the effects of surfactant proteins more visible. To test this hypothesis, we added increasing amounts of the PS peptide SP-$B_{1\text{-}25}$ into the CLSE preparations to measure how this peptide affects lipid dynamics in CLSE. This allowed us to change the P/L ratio of the samples enough to noticeably affect the bulk behavior of the lipids to develop a model of how lower levels of SP-B may traffic lipids. An initial test adding 5 mol% SP-$B_{1\text{-}25}$ to either $CLSE^T$ or $CLSE^L$ containing DPPC-d_{62} indicated the peptide had identical, noticeable effects on lipid dynamics in both samples (Figure S-7). These data further indicate that we did not change the lipid phase behavior being studied by removal of the small amounts of SP-B and SP-C; even when 5 mol% SP-$B_{1\text{-}25}$ is added to the two CLSE environments they remain indistinguishable.

Table 2
Lipid phase transition temperatures in CLSE.

Sample	T_m (T_m of neat lipid)	Observed melting range
$CLSE^T$/DPPC-d_{62}	28.0 °C (41.4 °C)	15–30 °C
$CLSE^T$/POPC-d_{31}	19.5 (−2.4)	0–25
$CLSE^T$/POPG-d_{31}	21.8 (−2.0)	0–25
$CLSE^T$/POPE-d_{31}	22.0 (28.0)	5–25

3.5. Addition of SP-$B_{1\text{-}25}$ has similar effects on native and synthetic PS lipid mixtures

For more systematic studies of the effect of peptide addition, we employed $CLSE^L$ and $CLSE^S$ samples. Fig. 3 shows via ^2H NMR spectroscopy the concentration effects of this peptide on lipid dynamics in $CLSE^L$ and $CLSE^S$ near physiologic temperature (38 °C). Variable temperature spectra of the lipids as well as dePaked spectra and order parameter profiles at 40 °C are provided in the Supplementary Information (Figures S-8, S-9 and S-10). In $CLSE^L$, the T_m of DPPC-d_{62} increases from 28.3 to 39.1 °C with increasing peptide concentration from 0 to 5 mol%. The bulk properties of the mono-unsaturated lipids are much less affected, suggesting that the peptide facilitates phase separation, particularly in $CLSE^L$ where some phase separation already occurs as reported above. This interpretation is supported by the fact that for the mono-unsaturated lipids acyl chain ordering decreases slightly with peptide addition, as evidenced by a gradual narrowing of the ^2H NMR

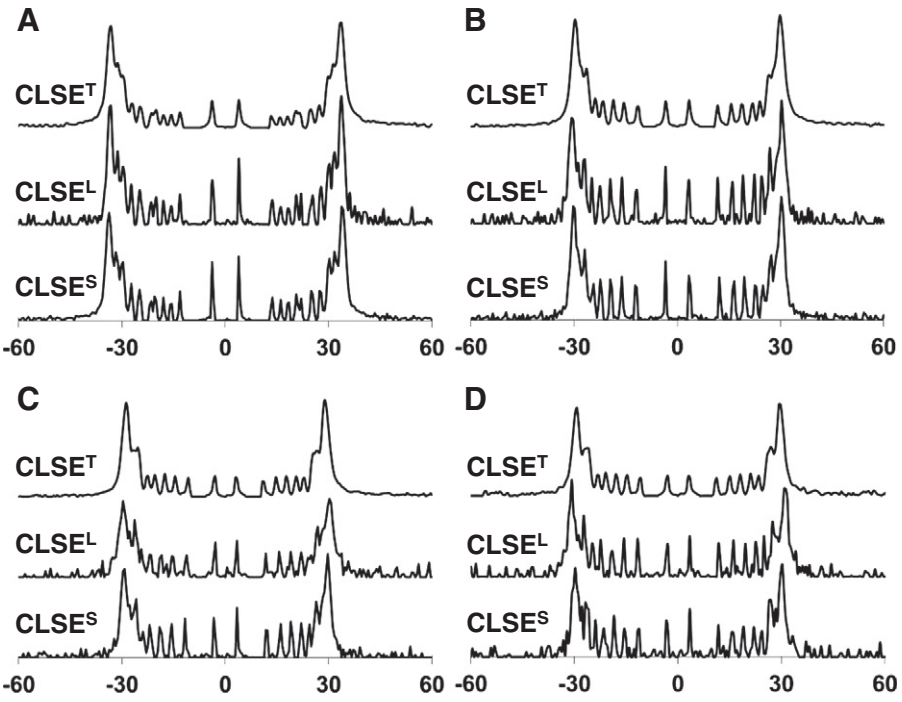

Fig. 2. Depaked ^{2}H NMR spectra for CLSE samples containing low reporter levels of A) DPPC-d_{62}, B) POPC-d_{31}, C) POPG-d_{31}, and D) POPE-d_{31} at 40 °C. At this temperature all the lipids are in the L_α phase, and the ordering of the individual lipid acyl chains within the different CLSE preparations is indistinguishable.

spectra, which would be consistent with a decrease in DPPC and/or cholesterol in association with the mono-unsaturated lipids. In both CLSE^L and CLSE^S lipid environments, exchange broadening is seen for DPPC at peptide concentrations of 3–5 mol% and physiologic temperature. This indicates that the DPPC dynamics in the synthetic PS mixture very closely mimic DPPC behavior in native PS, allowing facile, consistent testing of peptidomimetic effects on DPPC dynamics in a model system for developing PS replacement therapies. For POPC and POPG, the lipid dynamics in CLSE^L and CLSE^S are largely indistinguishable up to 3 mol% SP-$B_{1\text{-}25}$. However, at the highest concentration we tested, 5 mol%, the peptide is seen to also affect the bulk properties of the mono-unsaturated lipids in CLSE^S. This is consistent with our observations above that there are subtle lipid phase separation dynamics in native CLSE likely due to small amounts of species not added to the synthetic mixture, such as free fatty acids and lysolipids, or due to subtle differences in phospholipid and cholesterol concentrations relative to the CLSE^S we designed for this study. In summary, 1 mol% SP-$B_{1\text{-}25}$ does not appreciably affect lipid dynamics in either CLSE^L or CLSE^S environments at physiologic temperatures. At 3 mol% peptide the lipid phase behavior changes for DPPC-d_{62}, but not for POPC-d_{31} and POPG-d_{31}. At 5 mol% peptide, DPPC-d_{62} is most affected and overall the ^{2}H NMR spectra for DPPC-d_{62} exhibit the most change with increasing

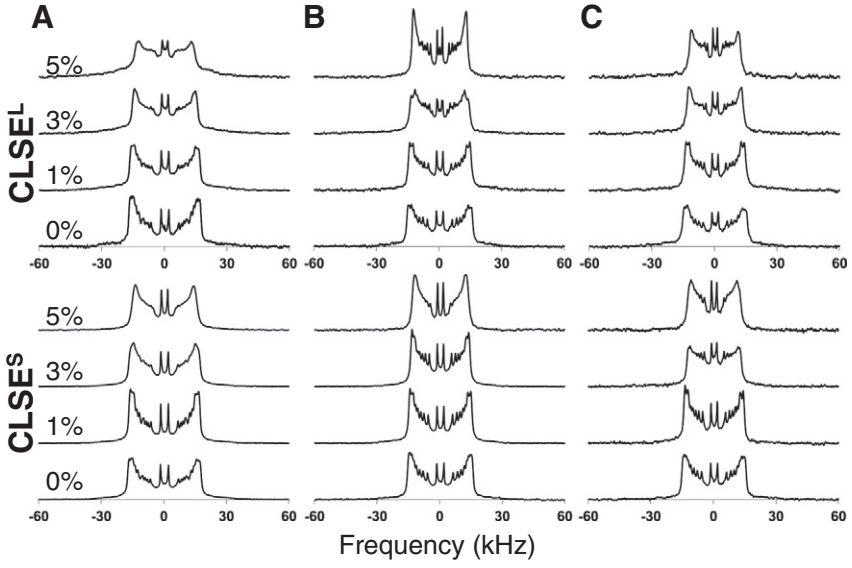

Fig. 3. Comparison via ^{2}H NMR spectroscopy of the effects of SP-$B_{1\text{-}25}$ addition on lipid dynamics at 38 °C in native CLSE (CLSE^L) lipids (top) vs. a synthetic (CLSE^S) lipid mixture (bottom) with the mol% of peptide indicated. The samples contain low reporter levels of A) DPPC-d_{62}, B) POPC-d_{31}, and C) POPG-d_{31} to monitor effects on the individual lipids. With peptide addition, a clear broadening in the lamellar lineshapes leading to a loss of resolution for the individual deuterated acyl chain positions in DPPC is seen in both lipid environments; in the synthetic mixture, the POPC and POPG lipids are also affected at the highest peptide concentration. This is likely due to less phase separation of DPPC in the synthetic lipid mixture.

concentration of SP-B_{1-25}, but POPC-d_{31} and POPG-d_{31} also exhibit non-lamellar phase lineshapes in $CLSE^S$.

3.6. The dynamics of DPPC on addition of SP-B_{1-25} to complex PS lipid mixtures indicate the formation of a new lipid phase

In previous studies of the effects of SP-B_{1-25} addition to binary 4:1 DPPC/POPG mixtures on lipid dynamics, we saw DPPC lineshapes at 1 mol% peptide that are very similar to those in $CLSE^L$ or $CLSE^S$ at 3 mol% peptide; at higher peptide concentration we saw the creation of an isotropic lipid phase in the binary lipid mixture (Fig. 4) [9]. While we do not see the onset of isotropic dynamics for DPPC-d_{62} in $CLSE^L$ or $CLSE^S$ at even 5 mol% peptide, the similarities of the DPPC-d_{62} lineshapes in $CLSE^L$ or $CLSE^S$ in losing sharp features for the individually deuterated positions in the acyl chain is likely due to the exchange of DPPC between lipid lamellae; the formation of an isotropic fluid phase is likely prevented by either the presence of cholesterol or the high percentage of mono-unsaturated lipids in the CLSE mixtures compared to 4:1 DPPC/POPG. To link our observations in this study to those of our previous work, we also examined DPPC dynamics in 8:2:1 DPPC/POPG/Chol. Fig. 4 shows ^2H NMR spectra of DPPC-d_{62} as a function of peptide concentration for the series of PS-like lipid mixtures of varying complexity. Order parameter profiles and variable temperature spectra are provided in Figures S-11 to S-14. Interestingly, in the ternary mixture the peptide is again observed to induce an isotropic phase which is in exchange with a broader component, suggesting that the induction of out-of-plane motions for DPPC is a hallmark of SP-B_{1-25} activity but that the higher concentration of mono-unsaturated lipids in CLSE may prevent the total conversation to a phase that is isotropic on the NMR timescale.

4. Discussion

The experiments delineated in this study had two major purposes. The first was to guide efforts in developing synthetic lipid/peptide formulations to replace CLSE and other animal derived lung surfactant formulations; the second was to better understand the molecular mechanisms underlying PS function. With research grade CLSE generously provided by ONY, Inc., we set out to systematically characterize the individual lipids in the CLSE environment and the effects of PS proteins and a peptide mimetic on their dynamics. In prior work we have shown that an analog of SP-B, SP-B_{1-25}, affects the dynamics of PS lipids in binary lipid systems, particularly the disaturated DPPC, as we observed isotropic ^2H ssNMR spectra for DPPC-d_{62} in 4:1 DPPC/POPG even at physiologic temperatures with the addition of 5 mol% SP-B_{1-25} [9]. With this evidence of the induction of unusual polymorphisms by SP-B_{1-25}, we proceeded to develop a model of lipid lamellae fusing together to form a fluid isotropic phase when greater amounts of the peptide are present. This model was supported by dynamic light scattering measurements showing the peptide-induced fusion of unilamellar vesicles. With this new perspective on possible lipid organization in PS, we asked whether such a model could apply to a clinically used, non-synthetic PS replacement therapy derived from a native source.

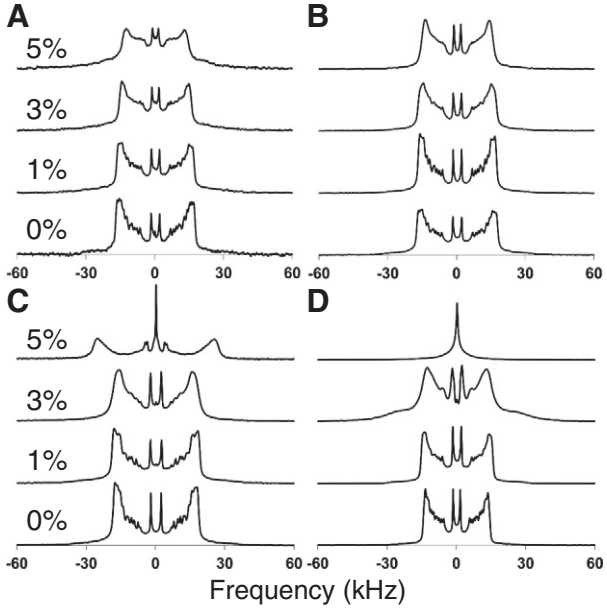

Fig. 4. A comparison of the effects of SP-B_{1-25} addition on DPPC dynamics at 38 °C in A) native CLSE lipids ($CLSE^L$), B) a synthetic lipid mixture mimicking CLSE, C) 8:2:1 DPPC/POPG/Chol ($CLSE^S$), and D) 4:1 DPPC/POPG. The spectra in D have been previously reported [9]. A clear change in DPPC dynamics with peptide addition is seen in all the lipid environments; it first appears as broadening in the lamellar lineshapes leading to a loss of resolution for the individual deuterated acyl chain positions and culminates in an isotropic lineshape in the simpler lipid mixtures.

Lung surfactant replacements currently used in clinical settings vary in origin, composition, and effect [31]. Animal derived PS formulations have been very successfully used to combat RDS in premature infants, but they raise concerns regarding purity, immunogenicity, and uniformity [16,32]. The experiments described in this work took advantage of a bovine PS source obtained via bronchiolar lavage, CLSE, which is analogous to the clinically used drug *Infasurf*, as it is the closest formulation to native surfactant available on the market [33]. One purpose of this study was to evaluate if a synthetic PS replacement formulation could exhibit properties similar to CLSE at the molecular level as a synthetic replacement would be ideal for treatment of RDS as it is more stable and has a longer shelf-life in addition to removing the risks of immune response and infection with animal sources of PS. To this end, we systematically characterized the organization and dynamics of the major individual lipid species in native CLSE and a synthetic lipid mixture designed to mimic CLSE.

Our initial characterization of CLSE via ^2H ssNMR showed that the phase behaviors of deuterated lipids in $CLSE^T$ are similar and exhibit a broad phase transition range. The broad T_m range from 10 to 30 °C is consistent with what has been observed in DSC traces of PS extracts [29]. While only lamellar lipid phases were observed, the T_m for DPPC was higher than for the monounsaturated lipids, suggesting phase separation, and led us to further investigate the CLSE lipids without protein present to examine whether the lipids in $CLSE^T$ (the therapeutic formulation containing SP-B and SP-C) and $CLSE^L$ (CLSE after protein removal) behaved similarly, which they did. This led us to examine whether a fully synthetic lipid mixture based on the main lipids of CLSE, $CLSE^S$, would also behave similarly. At physiologic temperatures, the major lipids in the three lipid systems exhibited identical properties. However, the phase separation of DPPC from the mono-unsaturated lipids at intermediate temperatures was not observed in $CLSE^S$, suggesting the importance of minor lipid species (such as free fatty acids) to the bulk properties of CLSE. In particular, palmitic acid, which is abundant in CLSE, melts at ~63 °C, contributing to a higher T_m for associated lipids [34]. Nonetheless, the similarity of the three lipid systems at physiologic temperatures suggests that $CLSE^S$ can serve as a well-controlled lipid system for evaluating peptidomimetics designed for use in PS replacement therapies; with the new insights we gained on phase separation, it is likely that small modifications can be made in the composition of $CLSE^S$, such as adding palmitic acid, allowing it to even more closely mimic native CLSE.

Unfortunately our studies using $CLSE^T$ did not yield particular insights into the role of SP-B in altering lipid dynamics at physiologic concentrations. This is likely due to the very small percentage of SP-B present in $CLSE^T$, at a P/L ratio of 1:1000. While a low protein concentration has proven effective in treating RDS, it does not measurably affect the bulk properties of the lipids enough to be seen by NMR spectroscopy experiments characterizing lipid dynamics. However, we note the P/L ratios in PS replacement therapies under development using synthetic

peptide analogs are substantially higher. For example, Surfaxin, the first FDA-approved peptide-based PS replacement therapy, has a P/L ratio of about 1:50 for KL_4, a synthetic peptide mimic of the C-terminus of SP-B. A peptide consisting of the first twenty-five amino acids of SP-B, SP-B_{1-25}, has also been demonstrated to retain the activity of full length SP-B as seen in both animal studies of lung function and air/water interface studies of surface tension at similarly higher concentrations [16]. Since our previous studies demonstrated that SP-B_{1-25} facilitates dynamics exchange between lipid lamellae leading to exchange broadening and non-lamellar lipid polymorphisms in simple binary lipid mixtures, we decided to use SP-B_{1-25}, which can be easily made with high purity, as a mimic of SP-B to assay how higher concentrations of a lipid-active peptide might affect lipid dynamics in either native CLSE or more complex synthetic lipid mixtures.

We observed that while SP-B_{1-25} affected the dynamics of all the lipids to some extent, DPPC displayed the largest changes in dynamics, particularly in $CLSE^T$; the mono-unsaturated phospholipids were much less affected. In all the lipid mixtures, peptide addition led to broadening of the DPPC lineshapes typical to lipids in a lamellar phase; at the highest percentages of peptide added (3–5 mol%), resolution of the individual deurated positions in the acyl chains was completely lost in both $CLSE^T$ and $CLSE^S$. In the simpler binary and ternary lipid mixtures, this broadening was seen at 1 mol% peptide and progressed to markedly changed lineshapes with major isotropic components at 3–5 mol% peptide concentrations. In our previous work using DPPC/POPG, we have shown that this exchange broadening for DPPC signals the onset of fusion of lipid lamellae culminating in an isotropic fluid phase. The fact that we see similar behavior in $CLSE^T$ suggests that peptide mediated exchange of DPPC between lipid lamellae is a hallmark of SP-B_{1-25} and may be important to its function in PS activity; It is notable that we do not see similar changes in POPC dynamics in $CLSE^T$ but they are seen in $CLSE^S$. This suggests that PS components driving lipid phase separation, such as cholesterol or palmitic acid, may act synergistically with SP-B_{1-25} leading to the selective trafficking of DPPC between lipid leaflets in the complex PS lipid network seen in the aqueous subphase.

5. Conclusion

Lipid assemblies that undergo geometric rearrangement could have a significant impact on lipid transfer to the air/water interface in the lung. The underlying aqueous, protein-containing hypophase in PS has unusual physical properties due to low concentrations of surfactant proteins which aid in trafficking secreted PS to the surface film lining the alveoli. To date, most studies of PS have focused on the molecular properties of the monolayer phospholipid film at the air/water interface or have investigated low resolution images of intact surfactant, such as electron micrographs of rat intra-alveolar lung surfactant [35–38].

This study presents new insights pertaining to the aqueous PS reservoir below the air/water interface; using NMR spectroscopy and selectively deuterated lipids, we are able to exclusively characterize the behavior of individual lipid species found in PS. We find that DPPC is uniquely phase separated in native CLSE, regardless of whether physiologic concentrations of SP-B and SP-C are present. Using an SP-B mimic with known PS activity, SP-B_{1-25}, we are able to show that peptide addition to CLSE leads to unusual DPPC dynamics and further phase separation of DPPC into a unique lipid phase. We also show that a synthetic lipid mixture designed to mimic native PS can faithfully reproduce many of these observations, suggesting a straightforward approach for assaying the potential of peptidomimetic formulations in PS replacement therapy.

Acknowledgements

The assistance of Dr. Alfred Chung in peptide synthesis is gratefully acknowledged. The authors give special recognition to coauthor Dr. Frank Mills, who contributed greatly to the beginning of this work and passed away in 2011. This research was funded by the Gates Foundation (J.R.L.). We also acknowledge ONY, Inc. for providing us with research grade calf lung surfactant extract (CLSE).

Appendix A. Supplementary data

Supplementary data to this article can be found online at http://dx.doi.org/10.1016/j.bbamem.2014.05.012.

References

[1] L.A. Creuwels, L.M. van Golde, H.P. Haagsman, The pulmonary surfactant system: biochemical and clinical aspects, Lung 175 (1997) 1–39.
[2] R.H. Notter, Lung surfactants: basic science and clinical applications, vol. 149, CRC Press, 2000.
[3] A.G. Serrano, J. Perez-Gil, Protein–lipid interactions and surface activity in the pulmonary surfactant system, Chem. Phys. Lipids 141 (2006) 105–118.
[4] J. Goerke, Pulmonary surfactant: functions and molecular composition, BBA-Mol. Basis Dis. 1408 (1998) 79–89.
[5] S.A. Rooney, S.L. Young, C.R. Mendelson, Molecular and cellular processing of lung surfactant, FASEB J. 8 (1994) 957–967.
[6] W.R. Rice, V.K. Sarin, J.L. Fox, J. Baatz, S. Wert, J.A. Whitsett, Surfactant peptides stimulate uptake of phosphatidylcholine by isolated cells, BBA 1006 (1989) 237–245.
[7] V.C. Antharam, D.W. Elliott, F.D. Mills, R.S. Farver, E. Sternin, J.R. Long, Penetration depth of surfactant peptide KL_4 into membranes is determined by fatty acid saturation, Biophys. J. 96 (2009) 4085–4098.
[8] V.C. Antharam, R.S. Farver, A. Kuznetsova, K.H. Sippel, F.D. Mills, D.W. Elliott, E. Sternin, J.R. Long, Interactions of the C-terminus of lung surfactant protein B with lipid bilayers are modulated by acyl chain saturation, BBA-Biomembranes 1778 (2008) 2544–2554.
[9] R.S. Farver, F.D. Mills, V.C. Antharam, J.N. Chebukati, G.E. Fanucci, J.R. Long, Lipid polymorphism induced by surfactant peptide SP-B_{1-25}, Biophys. J. 99 (2010) 1773–1782.
[10] Z.D. Wang, O. Gurel, S. Weinbach, R.H. Notter, Primary importance of zwitterionic over anionic phospholipids in the surface-active function of calf lung surfactant extract, Am. J. Respir. Crit. Care Med. 156 (1997) 1049–1057.
[11] R. Veldhuizen, K. Nag, S. Orgeig, F. Possmayer, The role of lipids in pulmonary surfactant, BBA-Mol. Basis Dis. 1408 (1998) 90–108.
[12] P.L. Yeagle, The Structure of Biological Membranes, 2nd ed. CRC Press, 2004.
[13] W.R. Perkins, R.B. Dause, R.A. Parente, S.R. Minchey, K.C. Neuman, S.M. Gruner, T.F. Taraschi, A.S. Janoff, Role of lipid polymorphism in pulmonary surfactant, Science 273 (1996) 330–332.
[14] K. Raghavendran, D. Willson, R.N. Notter, Surfactant therapy for acute lung injury and acute respiratory distress syndrome, Crit. Care Clin. 27 (2011) 525–559.
[15] H. Zhang, Y.E. Wang, Q.H. Fan, Y.Y. Zuo, On the low surface tension of lung surfactant, Langmuir 27 (2011) 8351–8358.
[16] F. Bringezu, J.Q. Ding, G. Brezesinski, A.J. Waring, J.A. Zasadzinski, Influence of pulmonary surfactant protein B on model lung surfactant monolayers, Langmuir 18 (2002) 2319–2325.
[17] S.D. Revak, T.A. Merritt, M. Hallman, G. Heldt, R.J. Lapolla, K. Hoey, R.A. Houghten, C.G. Cochrane, The use of synthetic peptides in the formation of biophysically and biologically-active pulmonary surfactants, Pediatr. Res. 29 (1991) 460–465.
[18] C.G. Cochrane, S.D. Revak, Pulmonary Surfactant Protein-B (Sp-B) — structure–fFunction-relationships, Science 254 (1991) 566–568.
[19] C.G. Cochrane, S.D. Revak, Protein–phospholipid interactions in pulmonary surfactant — the B-Francis-Parker-Lectureship, Chest 105 (1994) S57–S62.
[20] L.M. Gordon, K.Y.C. Lee, M.M. Lipp, J.A. Zasadzinski, F.J. Walther, M.A. Sherman, A.J. Waring, Conformational mapping of the N-terminal segment of surfactant protein B in lipid using C-13-enhanced Fourier transform infrared spectroscopy, J. Pept. Res. 55 (2000) 330–347.
[21] M. Sarker, A.J. Waring, F.J. Walther, K.M.W. Keough, V. Booth, Structure of mini-B, a functional fragment of surfactant protein B, in detergent micelles, Biochemistry 46 (2007) 11047–11056.
[22] M. Gupta, J.M. Hernandez-Juviel, A.J. Waring, R. Bruni, F.J. Walther, Comparison of functional efficacy of surfactant protein B analogues in lavaged rats, Eur. Respir. J. 16 (2000) 1129–1133.
[23] S.B. Hall, Z.D. Wang, R.H. Notter, Separation of subfractions of the hydrophobic components of calf lung surfactant, J. Lipid Res. 35 (1994) 1386–1394.
[24] P.S. Chen, T.Y. Toribara, H. Warner, Microdetermination of phosphorus, Anal. Chem. 28 (1956) 1756–1758.
[25] W. Schaffner, C. Weissman, Rapid, sensitive, and specific method for determination of protein in dilute-solution, Anal. Biochem. 56 (1973) 502–514.
[26] R.S. Kaplan, P.L. Pedersen, Sensitive protein assay in presence of high-levels of lipid, Methods Enzymol. 172 (1989) 393–399.
[27] E. Sternin, H. Schafer, I.V. Polozov, K. Gawrisch, Simultaneous determination of orientational and order parameter distributions from NMR spectra of partially oriented model membranes, J. Magn. Reson. 149 (2001) 110–113.
[28] H.I. Petrache, S.W. Dodd, M.F. Brown, Area per lipid and acyl length distributions in fluid phosphatidylcholines determined by H-2 NMR spectroscopy, Biophys. J. 79 (2000) 3172–3192.

[29] K. Nag, K.M. Keough, M.R. Morrow, Probing perturbation of bovine lung surfactant extracts by albumin using DSC and ^{2}H-NMR, Biophys. J. 90 (2006) 3632–3642.
[30] Y.Y. Zuo, R.A.W. Veldhuizen, A.W. Neumann, N.O. Petersen, F. Possmayer, Current perspectives in pulmonary surfactant — inhibition, enhancement and evaluation, BBA-Biomembranes 1778 (2008) 1947–1977.
[31] A.E. Curley, H.L. Halliday, The present status of exogenous surfactant for the newborn, Early Hum. Dev. 61 (2001) 67–83.
[32] D.S. Strayer, M. Hallman, T.A. Merritt, Immunogenicity of surfactant. 2. Porcine and bovine surfactants, Clin. Exp. Immunol. 83 (1991) 41–46.
[33] O. Blanco, J. Perez-Gil, Biochemical and pharmacological differences between preparations of exogenous natural surfactant used to treat respiratory distress syndrome: role of the different components in an efficient pulmonary surfactant, Eur. J. Pharmacol. 568 (2007) 1–15.
[34] F.D. Gunstone, J.L. Harwood, F.B. Padley, The Lipid Handbook, Chapman and Hall, London; New York, 1986.
[35] A. Cruz, L.A. Worthman, A.G. Serrano, C. Casals, K.M.W. Keough, J. Perez-Gil, Microstructure and dynamic surface properties of surfactant protein SP-B/dipalmitoylphosphatidylcholine interfacial films spread from lipid–protein bilayers, Eur. Biophys. J. 29 (2000) 204–213.
[36] H. Bachofen, U. Gerber, P. Gehr, M. Amrein, S. Schurch, Structures of pulmonary surfactant films adsorbed to an air–liquid interface in vitro, BBA-Biomembranes 1720 (2005) 59–72.
[37] H. Fehrenbach, Alveolar epithelial type II cell: defender of the alveolus revisited, Respir. Res. 2 (2001) 33–46.
[38] A. Cruz, L. Vazquez, M. Velez, J. Perez-Gil, Effect of pulmonary surfactant protein SP-B on the micro- and nanostructure of phospholipid films, Biophys. J. 86 (2004) 308–320.